Forming giant vesicles with controlled membrane composition, asymmetry, and contents

David L. Richmond[a,1], Eva M. Schmid[b,1], Sascha Martens[c,d], Jeanne C. Stachowiak[e], Nicole Liska[c], and Daniel A. Fletcher[a,b,2]

[a]Graduate Group in Biophysics, University of California, Berkeley, CA 94720; [b]Department of Bioengineering, University of California, Berkeley, CA 94720; [c]Neurobiology Division, Medical Research Council Laboratory of Molecular Biology, Cambridge CB2 0QH, United Kingdom; [d]Max F. Perutz Laboratories, University of Vienna, Doktor Bohr-Gasse 9/3, 1030 Vienna, Austria; and [e]Sandia National Laboratories, Livermore, CA 94551

Edited by Josep Rizo, University of Texas Southwestern, Dallas, TX, and accepted by the Editorial Board April 19, 2011 (received for review November 2, 2010)

Growing knowledge of the key molecular components involved in biological processes such as endocytosis, exocytosis, and motility has enabled direct testing of proposed mechanistic models by reconstitution. However, current techniques for building increasingly complex cellular structures and functions from purified components are limited in their ability to create conditions that emulate the physical and biochemical constraints of real cells. Here we present an integrated method for forming giant unilamellar vesicles with simultaneous control over (*i*) lipid composition and asymmetry, (*ii*) oriented membrane protein incorporation, and (*iii*) internal contents. As an application of this method, we constructed a synthetic system in which membrane proteins were delivered to the outside of giant vesicles, mimicking aspects of exocytosis. Using confocal fluorescence microscopy, we visualized small encapsulated vesicles docking and mixing membrane components with the giant vesicle membrane, resulting in exposure of previously encapsulated membrane proteins to the external environment. This method for creating giant vesicles can be used to test models of biological processes that depend on confined volume and complex membrane composition, and it may be useful in constructing functional systems for therapeutic and biomaterials applications.

lipid bilayer | transmembrane protein | SNARE | microfluidic jetting | synthetic biology

Lipid bilayer membranes provide the archetypal organizing structure by which cells separate themselves from their environment and internally compartmentalize and transport molecules. At the molecular level, cellular membranes are a crowded mix of many different lipids and proteins, and their composition and organization are crucial to a broad range of cellular functions (1). In endo- and exocytosis (2, 3), apoptosis (4), signal transduction (5), and motility (6), membranes serve as substrates for the activity of specialized lipids, transmembrane proteins, and associated binding proteins. Moreover, cells use cycles of endo- and exocytosis to dynamically regulate cell membrane composition and area.

Significant progress has been made in identifying the functional role of membrane composition and organization in cells. However, the sheer complexity and redundancy that underlies cellular behavior has made it difficult to elucidate many fundamental mechanisms at work in biological processes at membranes. To address these issues, traditional cell biological approaches are increasingly being complemented by in vitro experiments aimed at reconstituting cellular behavior from a minimal system of components. For example, synthetic lipid vesicles have been used to study the necessary and sufficient protein machinery for membrane fusion (3, 7–10), membrane deformation by cytoskeletal proteins (11–13), and scission by membrane binding proteins (14, 15).

To capture the essential features of complex cellular processes by reconstitution, methods are required to assemble purified components in ways that more faithfully emulate real cells (16). For example, properties that are believed to influence membrane processes and are therefore desirable to control in reconstitutions include asymmetric lipid composition, insertion of membrane proteins, physical properties such as membrane tension, and fixed volumes for soluble proteins and other biochemical components (1, 17–19). Current techniques use spontaneous lipid transfer (20), peptide-induced fusion (21), centrifugation (22, 23), or microfluidics (24, 25) to accomplish either controlled membrane composition or encapsulation of biomolecules in cell-sized volumes; however, formation of populations of monodisperse vesicles with unrestricted contents and user-defined membrane properties has not yet been demonstrated with existing techniques.

Here we present an integrated method for forming giant vesicles with controlled internal contents, asymmetric lipid composition, and oriented transmembrane proteins. We begin by demonstrating incorporation of physiologically relevant signaling lipids into giant unilamellar vesicles (GUVs) made by microfluidic jetting (26, 27), which enables simultaneous control of internal contents. We extend this approach to form GUVs with asymmetric lipid bilayers and then demonstrate incorporation and orientation of transmembrane proteins in the GUVs. Finally we combine key features of our method and demonstrate its utility by constructing a synthetic system in which lipid and transmembrane protein are delivered from encapsulated small unilamellar vesicles (SUVs) to GUV membranes using SNARE-family proteins (3, 7, 28). This demonstration mimics aspects of the dynamic regulation of plasma membrane properties by cells, and it provides a bioinspired mechanism for dynamically altering the surface chemistry of giant vesicles. The integrated method we present has the potential to facilitate both advanced reconstitution and construction of synthetic biological devices.

Results and Discussion

Formation of GUVs with Controlled Lipid Composition. A first step toward engineering systems that recapitulate the physical boundary conditions of cells is encapsulation of components in giant vesicles of controlled lipid chemistry. Several recent microfluidic techniques (22, 24–27) have achieved formation of giant vesicles with controlled contents using oil–water interfaces to define lipid membranes. However, these techniques form the membranes from lipids dissolved in oil and are incompatible with many biologically important lipids that display poor solubility in oil due to their net charge or saturated fatty acid tails. For example,

Author contributions: D.L.R., E.M.S., and D.A.F. designed research; D.L.R., E.M.S., and J.C.S. performed research; S.M. and N.L. contributed new reagents/analytic tools; D.L.R. and E.M.S. analyzed data; and D.L.R., E.M.S., and D.A.F. wrote the paper.

The authors declare no conflict of interest.

This article is a PNAS Direct Submission. J.R. is a guest editor invited by the Editorial Board.

[1]D.L.R. and E.M.S. contributed equally to this work.

[2]To whom correspondence should be addressed. E-mail: fletch@berkeley.edu.

This article contains supporting information online at www.pnas.org/lookup/suppl/doi:10.1073/pnas.1016410108/-/DCSupplemental.

the lipid phosphatidylinositol-4,5-bisphosphate (PIP_2) is involved in many essential signaling pathways but displays poor solubility in oil due to its strong negative charge.

To form giant vesicles with controlled contents, we first assembled a planar bilayer and then generated GUVs by microfluidic jetting. Planar lipid bilayers can be created at the interface between two aqueous droplets that are initially surrounded by oil (containing dissolved lipids) and then brought into contact, an approach pioneered by Bayley et al. to study membrane pores (29). We have previously demonstrated that these planar bilayers can be deformed by microfluidic jetting with a piezoelectric inkjet nozzle to form giant unilamellar vesicles (26). However, our previous use of lipids dissolved in oil prevented the inclusion of physiologically important signaling lipids.

To overcome this limitation, we formed planar bilayers with controlled lipid composition by delivering lipid content through the aqueous phase in the form of SUVs [modified protocol from Hwang, et al. (30)]. Using a custom acrylic chamber (Fig. 1*A* and Fig. S1) containing a small volume of oil, we kept the two aqueous droplets separated by a thin acrylic divider and loaded SUVs with the oil-insoluble lipid of interest into each droplet (Fig. 1*B*). The SUVs diffused within the droplets and gradually fused to the oil–water interface of each droplet, forming a continuous lipid monolayer around each droplet (Fig. 1*C*). When the divider was removed, the two droplets moved into contact and created a large (approximately 2 mm^2) planar bilayer membrane at their interface. Finally, giant unilamellar vesicles with controlled lipid composition were formed from this planar bilayer by microfluidic jetting (Fig. 1*C*). During this process, we attempted to minimize the residual oil in the planar lipid bilayer and resulting oil contamination of the GUVs (see *SI Text, GUV Formation by Microfluidic Jetting* and Fig. S2); however, we cannot fully exclude the possibility that oil molecules are present in the GUV membranes and may affect membrane properties such as rigidity and tension.

We used this procedure to incorporate fluorescently labeled PIP_2 (TMR-PIP_2) into giant vesicles (Fig. 1*D*). Confocal microscopy confirmed PIP_2 delivery to the GUV membrane. We also tested the generality of this protocol by incorporating functionalized lipids with large poly(ethylene glycol) (PEG) chains (1,2-distearoyl-*sn*-glycero-3-phosphoethanolamine-N-[PEG2000-N'-carboxyfluorescein]; see Fig. S3) and charged Ni-chelating head groups (1,2-dioleoyl-*sn*-glycero-3-[(N-(5-amino-1-carboxypentyl)-iminodiacetic acid)succinyl]) (DGS-NTA-Ni) (see Fig. 2). Both of these lipid species exhibit poor solubility in oil.

Alternatively, planar membranes can be formed from a combination of lipids dissolved in oil and oil-insoluble lipids added via SUVs to the aqueous droplets. GUVs made from these bilayers will contain both oil-insoluble and oil-soluble lipids, but they will lack controlled composition. This approach can be used to minimize background SUV concentration, and it may be most appropriate for doping in signaling lipids, which typically comprise <1% of the total phospholipid content of cellular membranes (1).

Formation of GUVs with Asymmetric Membranes. In addition to complex composition, cellular membranes are generally asymmetric in nature, maintaining a different environment on their cytosolic and extracellular sides. To mimic this fundamental feature of cellular membranes, we independently controlled the lipid composition in each leaflet of the unilamellar vesicle. Asymmetric planar bilayers can be formed as described above by incorporating different SUVs into each of the aqueous droplets (30) or by loading SUVs into one droplet and allowing lipids soluble in oil to form the monolayer of the second droplet. We formed giant vesicles with asymmetric membranes from the asymmetric planar bilayers again by microfluidic jetting. Because the continuity of the membrane is maintained during the vesicle formation process, the internal leaflet of the GUV originated from the lipid monolayer coating the droplet nearest the inkjet nozzle (inner droplet), and the external leaflet of the GUV came from the lipid monolayer coating the far droplet (outer droplet) (Fig. 2). In this way, inner and outer leaflet composition could be independently defined.

We demonstrated this method for formation of GUVs with asymmetric membranes by selectively incorporating oil-insoluble Ni-chelating lipids into the inner or outer leaflet of the bilayer. We confirmed the orientation of the Ni-chelating lipids using localization of 6x-His tagged green fluorescent protein (His-GFP), which has a high affinity for Ni, as a read-out. When SUVs containing Ni-chelating lipids were added to the inner droplet, encapsulated His-GFP localized to the GUV membrane; however, His-GFP added to the external solution did not (Fig. 2*A*). Conversely, when SUVs containing Ni-chelating lipids were added to the outer droplet, His-GFP added to the external

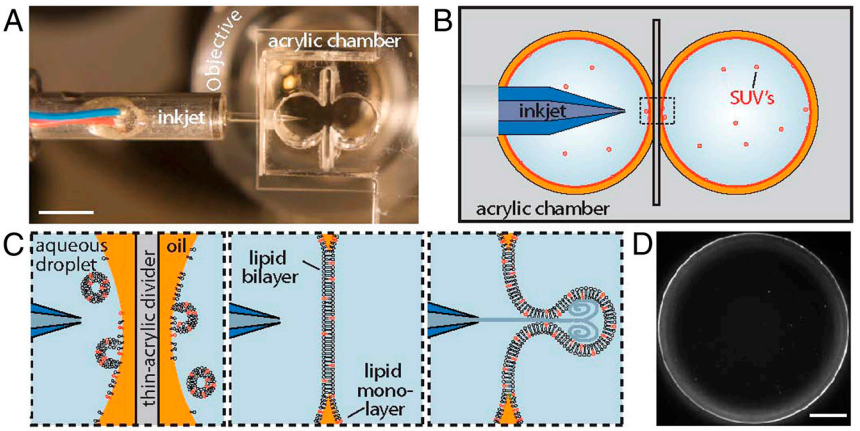

Fig. 1. GUVs with oil-insoluble lipids were formed by SUV incorporation into planar bilayers followed by microfluidic jetting. (*A*) A custom acrylic chamber was used to form giant vesicles by microfluidic jetting with a piezoelectric inkjet. The chamber was mounted on a microscope stage, and the inkjet device was inserted from a port in the side of the chamber. For image clarity, this chamber does not contain oil or aqueous droplets. Scale bar, 4 mm. (*B*) Aqueous droplets containing SUVs with oil-insoluble lipids (red) were incubated in the acrylic chamber containing oil. A thin acrylic divider separates the two aqueous droplets. (*C*) SUVs diffuse within the water droplet until they contact and fuse to the oil/water interface, forming a continuous lipid monolayer around each droplet. Removal of the thin acrylic divider allows the two droplets to move together and exclude oil between them. When the two lipid monolayers come into contact, they form a planar lipid bilayer. GUVs were formed by microfluidic jetting with the inkjet device that deforms the planar bilayer into a vesicle. Repeated pulsing of the inkjet results in the formation of multiple monodisperse vesicles. (*D*) TMR-PIP_2 was incorporated into a GUV by this method and imaged by confocal microscopy. Scale bar, 50 μm.

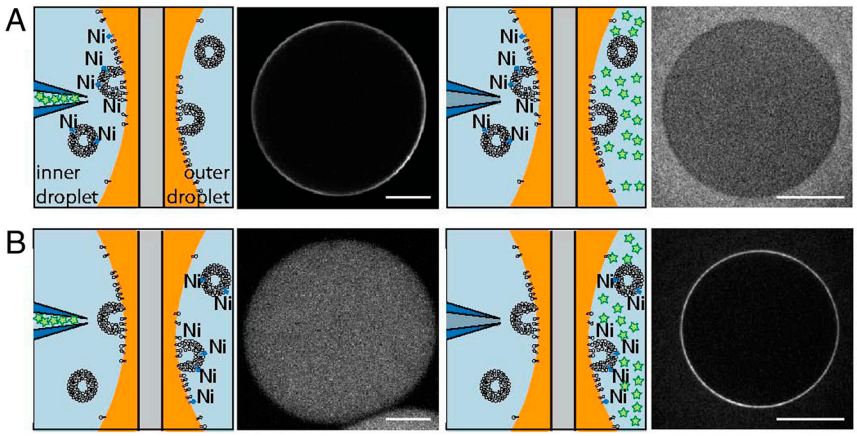

Fig. 2. GUVs with asymmetric lipid composition can be formed by controlling the SUV content of each reservoir. (*A*) SUVs containing Ni-chelating lipids were incubated in the droplet nearest the inkjet (inner droplet). His-GFP (green star) was either encapsulated in a GUV by microfluidic jetting (*Left*), or added to the outer droplet (*Right*), and the distribution of His-GFP was observed by confocal microscopy. (*B*) SUVs containing Ni-chelating lipids were incubated in the droplet furthest from the inkjet (outer droplet). His-GFP was either encapsulated in a GUV by microfluidic jetting (*Left*), or added to the outer droplet after vesicle formation (*Right*). All scale bars, 50 μm.

solution localized to the GUV membrane, whereas encapsulated His-GFP did not (Fig. 2*B*). This confirms the selective incorporation of Ni-chelating lipids into the inner or outer leaflet of the GUV. Whereas flipping of lipids from one leaflet to the other can occur over long times [many hours to days (31)], we did not observe significant lipid flip-flop over the timescale (approximately 1 h) of our experiments (Fig. S4).

Incorporation of Transmembrane Proteins and Control of Orientation in GUVs. A fundamental feature of cellular membranes and a central challenge for cellular reconstitutions is the abundant presence of transmembrane (TM) proteins (32). It has proven technically difficult to incorporate purified TM proteins into GUV membranes for reconstitution experiments. We overcome this difficulty through an extension of the SUV delivery method, using the well-characterized SNARE protein synaptobrevin (Syb) for a proof of principle experiment. A GFP fusion of synaptobrevin (GFP-Syb) was first incorporated into SUVs by the standard protocol of detergent-assisted insertion (33). Planar bilayers were formed from droplets containing SUVs with GFP-Syb, and GUVs with GFP-Syb were made by microfluidic jetting. The GUVs displayed bright, uniform fluorescence along their membrane, suggesting successful incorporation of the transmembrane protein (Fig. 3*A*).

As a second example of protein insertion into membranes, we formed GUVs containing the transmembrane protein syntaxin precomplexed with SNAP25 (tSNARE complex). We simultaneously tested incorporation of the tSNARE complex and its functionality by adding a water-soluble (truncated) version of synaptobrevin connected to GFP (SybSN-GFP). We observed strong localization of SybSN-GFP to the membrane, indicating successful incorporation of the tSNARE complex into the GUV membrane and formation of functional SNARE complexes (Fig. 3*B* and Fig. S5). No membrane localization of SybSN-GFP was detected in the absence of incorporated tSNAREs (Fig. 3*B*).

Many transmembrane proteins must be properly oriented to carry out their cellular function. For example, synaptobrevin is found in synaptic vesicle membranes with its hydrophilic SNARE domain oriented into the cytosol. Orientation of transmembrane proteins is accomplished by cells during insertion into the membrane, but reconstitution techniques are typically unable to achieve oriented insertion. Whereas the detergent-assisted insertion of Syb into SUVs is largely random, leading to approximately 50% of the protein oriented outward and 50% oriented inward (33), we set out to control protein orientation to emulate the physiological geometry in our GUVs. Therefore, we incubated GFP-Syb SUVs in the inner droplet [Fig. 3*C* (i)], where the microfluidic jet is inserted to form GUVs, and protein-free SUVs in the outer droplet. Orientation was measured by a fluorescence protease protection assay that works by probing the accessibility of the fluorescently labeled domain of a transmembrane protein to a membrane impermeable protease added to the external solution (34). We conducted this assay for GUVs formed from planar bilayers made by incubating GFP-Syb SUVs in three different configurations: (*i*) only the inner droplet, (*ii*) both droplets, or (*iii*) only the outer droplet (Fig. 3*C*). The fraction of GFP-Syb with a given orientation was calculated from the ratio of the fluor-

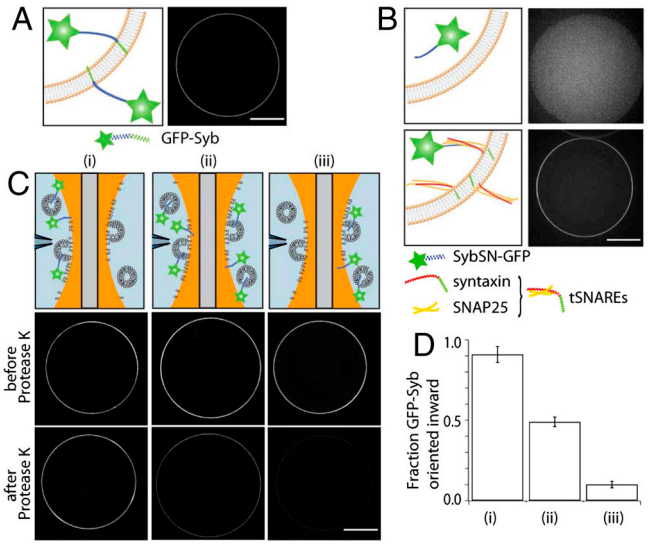

Fig. 3. Membrane proteins can be incorporated into GUVs with controlled orientation. (*A*) GFP-Syb was incorporated into GUVs and imaged by confocal microscopy. (*B*) SybSN-GFP (lacking the transmembrane domain) was encapsulated into (*Upper*) GUVs lacking tSNARE, and (*Lower*) GUVs containing tSNAREs. (*C*) (*Top*) Cartoons of the experimental setup. (*Middle*) GUVs made by microfluidic jetting of planar bilayers generated by GFP-Syb SUVs incubated in (*i*) the inner droplet, (*ii*) both droplets, or (*iii*) the outer droplet. (*Bottom*) The same GUVs were imaged again after the addition of Protease K, which degrades exposed protein, to the external medium. (*D*) GUVs made by incubating GFP-Syb SUVs in (*i*) the inner droplet had $91 \pm 5\%$ (SEM, $n = 4$ bilayers) GFP-Syb molecules oriented inward, (*ii*) both droplets had $49 \pm 3\%$ (SEM, $n = 4$ bilayers) GFP-Syb molecules oriented inward, and (*iii*) the outer droplet had $10 \pm 2\%$ (SEM, $n = 6$ bilayers) GFP-Syb molecules oriented inward. All scale bars, 50 μm.

escence intensity, measured by fluorescence microscopy, before and after addition of Protease K (see *SI Text*, *Analysis of TM Protein Orientation* and Fig. S6). Quantification of this data revealed that in configuration (*i*) $91 \pm 5\%$ (SEM, $n = 4$ bilayers), in (*ii*) $49 \pm 3\%$ (SEM, $n = 4$ bilayers), and in (*iii*) $10 \pm 2\%$ (SEM, $n = 6$ bilayers) of GFP-Syb was oriented inward, therefore confirming control over the orientation of incorporated transmembrane protein in GUVs (Fig. 3*D*). GFP-Syb orientation was stable over many hours (Fig. S7).

We achieved control of GFP-Syb orientation in GUVs by forming lipid monolayers that were destined for either the inner or outer leaflet of the vesicle and by capitalizing on the intrinsically asymmetric nature of GFP-Syb. Synaptobrevin has a single hydrophobic alpha-helix (transmembrane domain) connected to the water-soluble SNARE domain. The differing affinity of these two domains for the oil-water interface of the aqueous droplet likely specified the protein orientation, thus defining the polarity of the protein in the planar bilayer and consequently the GUV formed by microfluidic jetting. Connecting the SNARE domain to the globular protein GFP likely enhanced the orientation of the protein at the oil-water interface. In general, attachment of a water-soluble domain to a transmembrane protein of interest could be used as an engineering tool for orienting transmembrane proteins lacking large hydrophilic domains. If these proteins are connected to a fluorescent protein domain at a cytosolic-facing location by a linker containing a specific cleavage site, the engineered domain could be used to bias the orientation of the protein in the vesicle, confirm control of orientation by the fluorescence protease protection assay, and recover the native protein by cleavage. In general, asymmetric incorporation of transmembrane proteins into GUVs will also require a protein-specific assay to ensure functionality.

Dynamic Regulation of GUV Composition by SUV-GUV Membrane Mixing. Thus far, we have demonstrated the ability to form GUVs with controlled lipid composition, bilayer asymmetry, and oriented transmembrane proteins. To test the utility of this technique for experiments that depend on membrane composition and defined internal contents, we used the SNARE-fusion machinery to dynamically regulate GUV composition by SUV-GUV membrane mixing in a configuration that closely mimics the physiological geometry of exocytosis in cells. We loaded the inkjet with SUVs containing Syb (dark Syb and GFP-Syb at a 1 : 1 stoichiometry for detection) (vSNARE-SUVs) and the C2AB domain of the calcium-sensitive, synaptotagmin-related protein Doc2b. This solution was jetted into GUVs containing functional tSNARE complexes by deformation of a tSNARE-containing planar bilayer (Fig. 4*A*). We added $CaCl_2$ to the aqueous droplets surrounding the planar membrane, but not to the inkjet solution, so that when we formed GUVs, entrainment of $CaCl_2$ from the surrounding fluid initiated the activity of Doc2b at the exact moment of encapsulation within the GUV (35). Control experiments were performed equally with GUVs containing only syntaxin, and protein-free GUVs.

Addition of calcium-activated Doc2b caused vSNARE-SUVs to form clusters that diffused slowly ($D < 1\ \mu m^2/s$). Cluster formation by the synaptotagmin-related Doc2b is likely due to the two linked C2 domains binding to two apposing SUV membranes (Fig. 4*B*) (36, 37). By simply watching SUV clusters diffuse within the GUVs, we were able to observe two classes of events. In the first case, SUV clusters contacted the inner leaflet of the GUV membrane, and their diffusional motion was abruptly confined to the surface of the GUV, indicative of vesicle docking (Fig. 4*C* and Movie S1). The SUV clusters remained docked for the duration of observation, as demonstrated by persistent fluorescence on the GUV membrane (Fig. 4*C*). In the second case, we observed SUV clusters contacting the inner leaflet of the GUV membrane and immediately disappearing from sight (Fig. 4*D* and Movie S2). We

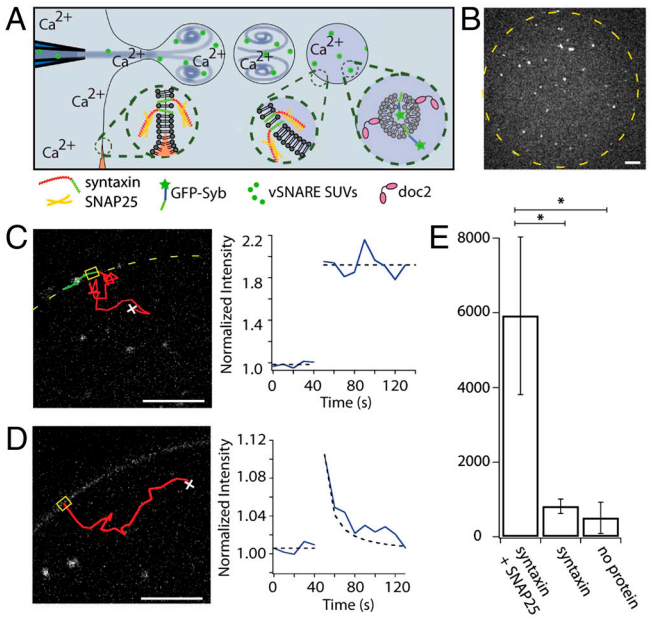

Fig. 4. Membrane mixing leads to transfer of SNARE proteins from SUVs to GUV membranes. (*A*) GUVs were formed with incorporated tSNAREs and encapsulated Doc2 and vSNARE-SUVs. Ca^{2+} was entrained from the aqueous droplets during the formation process. (*B*) Confocal image of vSNARE-SUVs encapsulated in a tSNARE-GUV (*C*) Docking of an SUV cluster to a GUV. Diffusion of an encapsulated SUV cluster was tracked for 10 min. The location of the SUV cluster in the first frame is denoted by "*x*." The track is separated into before (red) and after (green) docking to the GUV membrane. Fluorescence intensity of the GUV membrane at the docking location (yellow box) is shown for 2 min around the docking event. (*D*) Membrane transfer from an SUV cluster to a GUV membrane. The path of an SUV cluster was tracked (red) for 5 min, until it contacted the GUV membrane. The location of the SUV cluster in the first frame is denoted by "*x*." Fluorescence intensity of the GUV membrane at the contact location (yellow box) is shown for 2 min around the time of contact. Fluorescence decay is fit by a 2D diffusion model ($R^2 = 0.81$). (*E*) Transfer of GFP-Syb to the external leaflet of the GUV membrane was confirmed by addition of a fluorescently labeled antibody against GFP to the external solution. Fluorescence intensity of GUV membranes containing syntaxin + SNAP25 (tSNAREs) increased by 5922 ± 2108 a.u. (SEM, $n = 6$ bilayers), whereas GUV membranes containing only syntaxin, or no SNARE proteins, increased by 816 ± 193 a.u. (SEM, $n = 7$ bilayers) and 506 ± 419 a.u. (SEM, $n = 5$ bilayers), respectively. $^*p < 0.05$ (Student's *t* test). All scale bars, 25 μm.

again calculated the membrane fluorescence intensity at the contact site (Fig. 4*D*), and in contrast to docking, the local fluorescence intensity spike at the membrane steadily decayed to the baseline value, indicating that SUV-GUV membrane mixing occurred. We further analyzed the fluorescence decay after contact and found that both the timescale and decay shape are consistent with 2D diffusive mixing within the GUV membrane (see *SI Text*, *Analysis of SUV-GUV Docking and Membrane Mixing* and Fig. S8). We also confirmed that these events were not due to vertical diffusion out of the observed volume by tracking the vertical position of these punctae (Fig. S9). In control experiments where we do not incorporate tSNAREs into the GUV membrane, we observe only docking but no membrane mixing ($n = 10$ independent experiments).

In this geometry, cumulative SUV-GUV membrane mixing events should result in changing GUV membrane composition and presentation of vSNARE-GFP molecules from the GUV surface. Consistent with this hypothesis, we found that the overall GUV membrane increased in fluorescence over time for tSNARE-containing GUVs, indicating that GFP-Syb was transferred to the GUV membrane (Fig. S10). To confirm presentation of GFP-Syb from the external surface of GUVs, we added a fluorescently labeled GFP antibody (αGFP-AF594) to the exter-

nal solution and observed a significant increase in antibody fluorescence for GUVs containing the complete SNARE fusion machinery. This suggests a SNARE-dependent membrane mixing process (Fig. 4*E*); however, we cannot exclude the possibility that residual detergent and decane destabilized the membranes and facilitated membrane mixing by SNAREs.

Conclusions

Cellular reconstitutions are limited by the technical challenge of assembling giant vesicles with controlled internal contents and complex bilayer properties. Recently, progress has been made to encapsulate macromolecules in cell-sized volumes using strategies that rely on lipids dissolved in oil for assembling lipid bilayers, which limits control of membrane composition and organization. Here we have demonstrated a technique that addresses this challenge, enabling assembly of vesicles with simultaneous control of internal contents and membrane properties, including asymmetric distribution of physiological lipids and transmembrane proteins. The technique we use, microfluidic jetting, requires more specialized equipment than other approaches such as inverted emulsions, but it separates the process of vesicle formation from that of bilayer formation, allowing monitoring and minimization of oil contamination in the bilayer. We anticipate that the technique we describe will be especially useful for facilitating reconstitutions that involve membrane interactions, such as exocytosis and endocytosis, antigen presentation, viral entry, and signal transduction. Presentation of proteins on the external surface of GUVs by SUV-GUV membrane mixing mimics the process by which cells dynamically regulate their membrane composition, suggesting the potential for engineering a device that, similar to antigen presenting cells, presents specific surface chemistry in response to external cues. The ability to engineer synthetic lipid vesicles with cellular controls will further efforts to construct bioinspired devices for therapeutic and active biomaterials applications.

Materials and Methods

Additional information on SUV preparation, protein expression, proteo-liposome preparation, chamber design, planar bilayer formation, GUV formation by microfluidic jetting, image acquisition, and analysis is available in *SI Text*.

Incorporating TMR-PIP$_2$ into GUVs. Aqueous droplets containing 0.1 mg/mL DPhPC/TMR-PIP$_2$ SUVs were added to both sides of the oil-loaded chamber, and the chamber was incubated overnight at 4 °C. The thin acrylic divider was removed, and the chamber was left for 10 min to allow for planar bilayer formation before an inkjet loaded with 350 mOsm sucrose was used to form GUVs by microfluidic jetting.

Asymmetric DGS-NTA-Ni GUV experiment. To selectively incorporate DGS-NTA-Ni into the inner leaflet of a GUV the oil-containing chamber was set up with an inner droplet containing 0.02 mg/mL DPhPC/DGS-NTA-Ni SUVs and an outer droplet containing 0.02 mg/mL DPhPC SUVs, and was incubated for 1 h. After incubation, DPhPC in oil was added to a final concentration of 21 mg/mL in the chamber. The thin acrylic divider was removed and GUVs were formed using an inkjet containing either 2 μM His-GFP and 6% iodixanol in 10 mM Hepes pH 7.5, 200 mM KCl (Fig. 2*A*, *Left*), or only 6% iodixanol in 10 mM Hepes pH 7.5, 200 mM KCl (Fig. 2*A*, *Right*). After formation of multiple GUVs from a single bilayer, the sample was transferred to a spinning disc confocal microscope for imaging. GUVs with encapsulated His-GFP were imaged immediately. 0.3 μM His-GFP was added to chambers with GUVs lacking encapsulated His-GFP, and they were incubated for 30 min before imaging. Selective incorporation of DGS-NTA-Ni into the outer leaflet of a GUV was accomplished by repeating this procedure, with 0.02 mg/mL DPhPC/DGS-NTA-Ni SUVs in the outer droplet and 0.02 mg/mL DPhPC SUVs in the inner droplet (Fig. 2*B*).

Incorporation of tSNAREs and Functional SNARE Complex Formation. Aqueous droplets containing either 0.05 mg/mL tSNARE SUVs (DPhPC SUVs with inserted tSNARE complexes) and 0.05 mg/mL supplement SUVs (DPhPC/DPhPS/cholesterol 70/20/10) or 0.1 mg/mL supplement SUVs only (control), in 25 mM Hepes pH 7.5, 100 mM KCl, 2 mM DTT were added to both sides of an oil-loaded chamber, and the chamber was incubated overnight at 4 °C. After incubation, DPhPC in oil was added to a final concentration of 21 mg/mL in the chamber. The thin acrylic divider was removed, forming a tSNARE-containing planar bilayer, and an inkjet loaded with 1 μM SybSN-GFP, 6% iodixanol, 25 mM Hepes pH 7.5, 100 mM KCl and 2 mM DTT was used to form GUVs. Alternatively, binding of SybSN-GFP to tSNAREs in the external leaflet of GUVs was tested by addition of 1 μM SybSN-GFP to the chamber after vesicle formation, instead of loading it into the inkjet.

GFP-Syb Incorporation and Orientation. To form GUVs with GFP-Syb with the GFP domain facing outward the oil-containing chamber was set up with an outer droplet containing 0.05 mg/mL GFP-Syb SUVs and an inner droplet containing 0.05 mg/mL DPhPC SUVs and incubated overnight at 4 °C. After incubation, DPhPC in oil was added to a final concentration of 21 mg/mL in the chamber. The thin acrylic divider was removed and an inkjet loaded with 6% iodixanol, 25 mM Hepes pH 7.5, 100 mM KCl and 2 mM DTT was used to form GUVs. After formation of multiple GUVs from a single bilayer, images of the GUVs were captured using spinning disc confocal microscopy and positions were recorded using a motorized stage (Prior). Protease K (Sigma–Aldrich) was carefully added to the outer droplet to a final concentration of 0.2 mg/mL, and mixed by gentle pipetting. Protease K was added approximately 1 h after vesicle formation, unless we tested for stability of protein orientation, in which case we waited 9 h before addition of protease K. After 10 min of incubation we returned to the previously recorded positions and captured a second set of images of the same GUVs.

Conversely, GFP-Syb was incorporated into GUVs with the GFP domain facing inward by setting up the oil-containing chamber with 0.05 mg/mL GFP-Syb SUVs in the inner droplet, and 0.05 mg/mL DPhPC SUVs in the outer droplet for overnight incubation. GUVs with GFP-Syb oriented symmetrically were formed by incubating 0.05 mg/mL GFP-Syb SUVs in both droplets.

SUV-GUV Membrane Mixing Experiment. Aqueous droplets containing either 0.05 mg/mL tSNARE SUVs (DPhPC) and 0.05 mg/mL supplement SUVs (DPhPC/DPhPS/cholesterol 70/20/10) for membrane mixing experiments or 0.1 mg/mL supplement SUVs only for control experiments, in 25 mM Hepes pH 7.5, 100 mM KCl, 0.4 mM $CaCl_2$, 2 mM DTT were added to both sides of an oil-loaded chamber, and the chamber was incubated overnight at 4 °C. After incubation, DPhPC in oil was added to a final concentration of 21 mg/mL in the chamber. The thin acrylic divider was removed, forming a tSNARE-containing planar bilayer, and an inkjet loaded with 2 μg/mL vSNARE SUVs, 0.5 μM Doc2, 6% iodixanol, 25 mM Hepes pH 7.5, 100 mM KCl and 2 mM DTT was used to form GUVs.

For detection of GFP-Syb delivery from the inner leaflet of SUVs to the outer leaflet of GUVs we formed tSNARE-containing planar bilayers as described above. To control for nonspecific membrane mixing we formed planar bilayers from (1) SUVs containing syntaxin only, or (2) protein-free DPhPC SUVs. We encapsulated 20 μg/mL vSNARE SUVs, 0.5 μM Doc2, 6% iodixanol, 25 mM Hepes pH 7.5, 100 mM KCl and 2 mM DTT. We incubated the GUVs for 12–16 h after formation, to ensure maximum membrane mixing and protein presentation. We then added 30 μg/mL anti-GFP AF 594 antibody (Invitrogen) to the surrounding solution, incubated for 30 min on room temperature, washed and imaged the GUVs with confocal microscopy. Linescan analysis was used to measure fluorescence increase due to antibody binding. For details of images acquisition and analysis of SUV-GUV docking and membrane mixing, see *SI Text* and Figs. S11 and S12.

ACKNOWLEDGMENTS. We thank Patrick Oakes, Ali Hanson, and Erkan Tuzel for their contributions and helpful suggestions for tracking vesicle diffusion and docking during the 2009 MBL Physiology Course in Woods Hole, MA. We also thank William Hwang for experimental advice about forming planar membranes from SUVs, and Ross Rounsevell for supplying His-GFP. D.L.R. acknowledges fellowship support from the Natural Sciences and Engineering Research Council of Canada. E.M.S. was supported by the Miller Institute for Basic Research in Science. Sandia is a multiprogram laboratory operated by Sandia Corporation, a Lockheed Martin Company, for the US Department of Energy's National Nuclear Security Administration under Contract DE-AC04-94AL85000. N.L. acknowledges fellowship support by the Austrian Academy of Sciences. This work was supported in part by the Cell Propulsion Lab, a National Institutes of Health Nanomedicine Development Center (D.A.F.).

1. Meer GV, Voelker DR, Feigenson GW (2008) Membrane lipids: Where they are and how they behave. *Nat Rev Mol Cell Biol* 9:112–124.

2. Paolo GD, Camilli PD (2006) Phosphoinositides in cell regulation and membrane dynamics. *Nature* 443:651–657.

3. Wickner W, Schekman R (2008) Membrane fusion. *Nat Struct Mol Biol* 15:658–664.
4. Fadok VA, et al. (1992) Exposure of phosphatidylserine on the surface of apoptotic lymphocytes triggers specific recognition and removal by macrophages. *J Immunol* 148:2207–2216.
5. Hannun YA, Obeid LM (2008) Principles of bioactive lipid signalling: Lessons from sphingolipids. *Nat Rev Mol Cell Biol* 9:139–150.
6. Vanhaesebroeck B, et al. (2001) Synthesis and function of 3-phosphorylated inositol lipids. *Annu Rev Biochem* 70:535–602.
7. Martens S, McMahon HT (2008) Mechanisms of membrane fusion: disparate players and common principles. *Nat Rev Mol Cell Biol* 9:543–556.
8. Hui E, Johnson CP, Yao J, Dunning FM, Chapman ER (2009) Synaptotagmin-mediated bending of the target membrane is a critical step in Ca(2+)-regulated fusion. *Cell* 138:709–721.
9. Tareste D, Shen J, Melia TJ, Rothman JE (2008) SNAREpin/Munc18 promotes adhesion and fusion of large vesicles to giant membranes. *Proc Natl Acad Sci USA* 105:2380–2385.
10. Ohya T, et al. (2009) Reconstitution of Rab- and SNARE-dependent membrane fusion by synthetic endosomes. *Nature* 459:1091–1097.
11. Liu A, et al. (2008) Membrane-induced bundling of actin filaments. *Nat Phys* 4:789–793.
12. Osawa M, Anderson DE, Erickson HP (2008) Reconstitution of contractile FtsZ rings in liposomes. *Science* 320:792–794.
13. Koster G, VanDuijn M, Hofs B, Dogterom M (2003) Membrane tube formation from giant vesicles by dynamic association of motor proteins. *Proc Natl Acad Sci USA* 100:15583–15588.
14. Wollert T, Wunder C, Lippincott-Schwartz J, Hurley JH (2009) Membrane scission by the ESCRT-III complex. *Nature* 458:172–177.
15. Roux A, Uyhazi K, Frost A, Camilli PD (2006) GTP-dependent twisting of dynamin implicates constriction and tension in membrane fission. *Nature* 441:528–531.
16. Liu A, Fletcher D (2009) Biology under construction: In vitro reconstitution of cellular function. *Nat Rev Mol Cell Biol* 10:644–650.
17. Antonny B (2006) Membrane deformation by protein coats. *Curr Opin Cell Biol* 18:386–394.
18. Lecuit T, Lenne P (2007) Cell surface mechanics and the control of cell shape, tissue patterns, and morphogenesis. *Nat Rev Mol Cell Bio* 8:633–644.
19. Gregoretti IV, Margolin G, Alber MS, Goodson HV (2006) Insights into cytoskeletal behavior from computational modeling of dynamic microtubules in a cell-like environment. *J Cell Sci* 119:4781–4788.
20. Pagano RE, Martin OC, Schroit AJ, Struck DK (1981) Formation of asymmetric phospholipid membranes via spontaneous transfer of fluorescent lipid analogues between vesicle populations. *Biochemistry* 20:4920–4927.
21. Kahya N, Pécheur EI, Boeij WPD, Wiersma DA, Hoekstra D (2001) Reconstitution of membrane proteins into giant unilamellar vesicles via peptide-induced fusion. *Biophys J* 81:1464–1474.
22. Pautot S, Frisken BJ, Weitz DA (2003) Production of unilamellar vesicles using an inverted emulsion. *Langmuir* 19:2870–2879.
23. Pautot S, Frisken BJ, Weitz DA (2003) Engineering asymmetric vesicles. *Proc Natl Acad Sci USA* 100:10718–10721.
24. Funakoshi K, Suzuki H, Takeuchi S (2007) Formation of giant lipid vesiclelike compartments from a planar lipid membrane by a pulsed jet flow. *J Am Chem Soc* 129:12608–12609.
25. Utada AS, et al. (2005) Monodisperse double emulsions generated from a microcapillary device. *Science* 308:537–541.
26. Stachowiak JC, Richmond DL, Li TH, Fletcher DF (2009) Inkjet formation of unilamellar lipid vesicles for cell-like encapsulation. *Lab Chip* 9:2003–2009.
27. Stachowiak JC, et al. (2008) Unilamellar vesicle formation and encapsulation by microfluidic jetting. *Proc Natl Acad Sci USA* 105:4697–4702.
28. Jahn R, Scheller RH (2006) SNAREs-engines for membrane fusion. *Nat Rev Mol Cell Biol* 7:631–643.
29. Bayley H, et al. (2008) Droplet interface bilayers. *Mol Biosyst* 4:1191–1208.
30. Hwang WL, Chen M, Cronin B, Holden MA, Bayley H (2008) Asymmetric droplet interface bilayers. *J Am Chem Soc* 130:5878–5879.
31. Homan R, Pownall HJ (1988) Transbilayer diffusion of phospholipids: Dependence on headgroup structure and acyl chain length. *Biochim Biophys Acta* 938:155–166.
32. Engelman DM (2005) Membranes are more mosaic than fluid. *Nature* 438:578–580.
33. Martens S, Kozlov MM, McMahon HT (2007) How synaptotagmin promotes membrane fusion. *Science* 316:1205–1208.
34. Lorenz H, Hailey DW, Wunder C, Lippincott-Schwartz J (2006) The fluorescence protease protection (FPP) assay to determine protein localization and membrane topology. *Nat Protoc* 1:276–279.
35. Li TH, Stachowiak JC, Fletcher DA (2009) Mixing solutions in inkjet formed vesicles. *Methods Enzymol* 465:75–94.
36. Groffen AJ, et al. (2010) Doc2b is a high-affinity Ca^{2+} sensor for spontaneous neurotransmitter release. *Science* 327:1614–1618.
37. Connell E, et al. (2008) Cross-linking of phospholipid membranes is a conserved property of calcium-sensitive synaptotagmins. *J Mol Biology* 380:42–50.